IJE TRANSACTIONS A: Basics Vol. 39, No. 10, (October 2026) 2472-2484

International Journal of Engineering

Journal Homepage: www.ije.ir

Justification of the Power-performance Characteristics of a Two-section Positive Displacement Motor with a Bi-rotary Mechanism

M. V. Dvoynikov, D. O. Morozov*

Well Drilling Department, Oil and Gas Faculty, Saint Petersburg Mining University, Saint Petersburg, Russia

PAPER INFO

Paper history:
Received 08 September 2025
Received in revised form 16 October 2025
Accepted 26 December 2025

Keywords:
Drilling
Directional Drilling
Positive Displacement Motor
Bi-rotary Mechanism
Power-performance Characteristics
Working Elements

ABSTRACT

For drilling oil and gas wells, screw downhole motors – also known as positive displacement motors (PDMs) – are widely used both in Russia and abroad, accounting for over 80% of applications. However, PDMs exhibit a number of drawbacks affecting the efficiency of directional and overall drilling. First, harmful dynamic phenomena are generated in the motor's power section, which adversely impact drilling performance. Second, the low output shaft speed prevents the use of certain diamond/PDC bits. Third, the ratio of horizontal reach to true vertical depth almost never exceeds 4.0, whereas with rotary steerable systems (RSS) it can reach 6.0. At present, both motorized and non-motorized RSS are being used with increasing frequency to drill wells with greater departure from vertical and precisely prescribed trajectory profiles at maximum step-out. It is known that each of these and other solutions has its own advantages and limitations that are difficult, and sometimes impossible, to eliminate during drilling operations. A drilling technology employing a two-section PDM with a bi-rotary mechanism is proposed to increase the efficiency of directional drilling. This work presents prototypes of the developed motor, identifies its characteristic similarities and differences relative to earlier tools and technologies, and determines the power-performance characteristics of the two-section PDM – namely torque, rotational speed, power at the bit, and the axial load generated within the bottomhole assembly. The feasibility of the regulating motor operation by adjusting the drilling fluid (DF) flow rate to the power section is substantiated. Potential topics for future research are outlined.

doi: *10.5829/ije.2026.39.10a.10*

Graphical Abstract

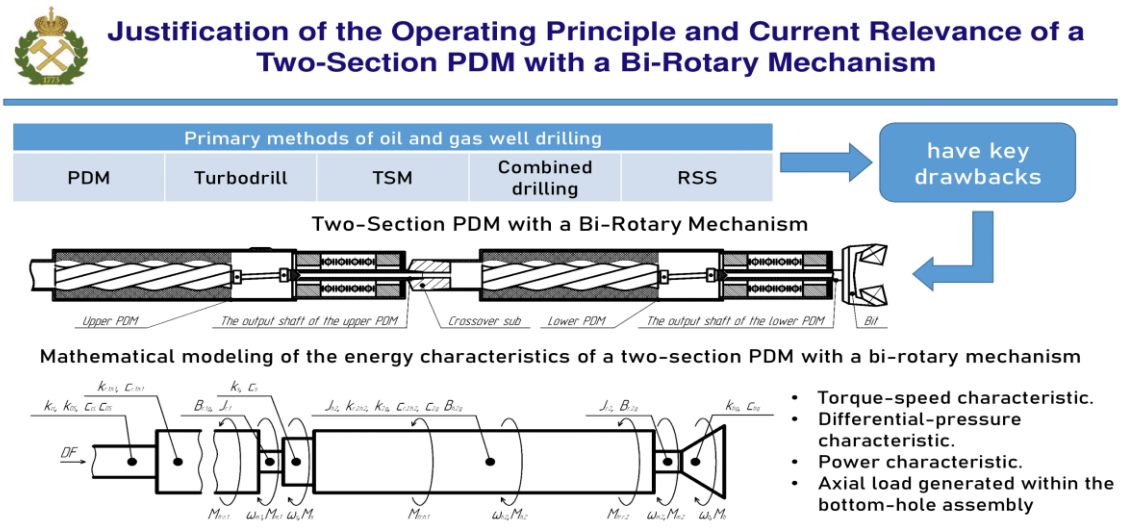

*Corresponding Author Email: dmitrij_morozov_01@mail.ru (D. O. Morozov)

Please cite this article as: Dvoynikov MV, Morozov DO. Justification of the Power-performance Characteristics of a Two-section Positive Displacement Motor with a Bi-rotary Mechanism. International Journal of Engineering, Transactions A: Basics. 2026;39(10):2472-84.

NOMENCLATURE

k	Torsional stiffness (N·m/rad)	v	Linear velocity (m/s)
z	Number of lobes of the WE	e	Eccentricity (m)
M	Torque characteristic (N·m)	L	Length of the PDM element (m)
P	Pressure drop (differential pressure) (Pa)	m	Rotor mass (kg)
Q	DF flow rate (m³/s)	R	Radius of the PDM element (m)
V	Working volume (m³/s)	N	Power characteristic (W)
E	Energy on the PDM element (J)	Rel	Rayleigh dissipation (N·m)
h	Moment arm of the forces generating the resistance torque (m)	**Greek Symbols**	
T	Stator helical surface pitch (m)	μ	Dynamic viscosity of the drilling fluid (Pa·s)
n	Rotational speed (rev/s)	τ	Output torque of the two-section PDM (N·m)
F	Force characteristic (N)	θ	Twist angle (rad)
c	Relative viscous loss coefficient on a PDM element (N·m·s/rad)	η	Efficiency (%)
B	Viscous loss coefficient on a PDM element (N·m·s/rad)	Λ	Number of contact lines of the working elements
J'	Polar moment of area (m⁴)	ω	Angular velocity (s⁻¹)
J	Moment of inertia (kg·m²)	$\dot{\omega}$	Angular acceleration (m/s²)

1. INTRODUCTION

The use of a PDM to drill long directional intervals while achieving the required curvature is constrained by the inability to deliver sufficient weight on bit (WOB). The operational capability of PDM-based directional drilling is reduced by friction forces acting between the drilling assembly and the formation. To transmit WOB to the bit, it is recommended to employ special tools installed in the drill string (DS) or to add lubricants to the DF. These measures typically increase the achievable length of oriented (sliding) directional drilling by no more than 500-1,000 m (1-3).

A further increase in the horizontal reach is possible only with additional rotation of the DS. However, rotation of the DS – and thus of the bent-housing PDM – precludes intentional trajectory deflection via oriented drilling (4). To improve the efficiency of directional intervals, in addition to the friction-reduction methods outlined above, the authors propose using a dynamic module implemented as the rotating housing of the lower motor in a two-section PDM based on a bi-rotary mechanism. The foregoing underscores the relevance of oriented directional drilling for complex well profiles – a challenge that can be addressed by developing a drilling methodology employing a two-section PDM with a co-rotating rotor-housing lower stage (two-section bi-rotor PDM).

Multi-section motors with rotors connected in series are known (1, 5). Their operating principle differs from that of a bi-rotary mechanism, which introduces specific operational considerations for the proposed motor. The most critical of these is selecting compatible motors so that the assembled two-section PDM not only performs efficiently but also avoids off-design and failure modes – since, as will be shown below, there is a high likelihood of one of the units entering a braking (stall) mode. The efficiency of drilling with a sectional PDM increases due to higher power at the rock-cutting tool (bit), yet the magnitude – and, in some cases, the very presence – of any gain in drilling performance (rate of penetration (ROP)) depends on the prevailing geologic and technical conditions. A known peculiarity of rock failure is that raising rotational speed (revolutions per minute (RPM)) at constant torque characteristics does not necessarily improve ROP. The feasibility of tuning PDM performance by varying DF flow rate through the bit is substantiated and contrasted with tuning via changes in surface DS RPM and applied WOB (6). With a special coupling of two PDMs, the housing of the lower motor functions as a dynamic module that reduces frictional interaction (drag) between the bottomhole assembly (BHA) and the borehole wall, promotes formation of a filter cake on the wellbore walls, and induces turbulence in the DF, thereby enhancing cuttings transport.

The study addresses the determination of drilling parameters for a two-section bi-rotor PDM (7) – namely torque, rotational speed, power, pressure drop, and the axial load generated within the BHA of the two-section PDM. A mathematical model was developed, the torque-speed characteristic of the proposed motor was computed, and a drilling methodology for the two-section bi-rotor PDM is described, neglecting the internally generated oscillations identified in this work.

1. 1. Analysis of Technical Solutions and Drilling Technologies for Directional and Horizontal Wells

The evolution of well construction has been underway for two centuries. The process of building a well – specifically, the technologies used to create a geometrically defined excavation – is governed by its intended purpose. As target depths, lateral reach, and the variety of transcendental curves employed in directional well design have grown, the approaches to selecting bit-drive systems and other equipment, as well as the methods for oriented trajectory deflection, have evolved accordingly (8-10).

To develop a mathematical model of the bo-rotor PDM and to understand its operating process, the design of a single-screw PDM is first considered. A PDM can be

viewed as an epicyclic (planetary-type) reduction mechanism with a stationary stator and a moving rotor – the conceptual opposite of a turbodrill. The helical rotor, having one lobe fewer than the stator, is set into rotation when DF is supplied into the high-pressure cavities.

The rotor and stator remain in continuous contact, and the number of contact lines along the working-element profiles equals the number of stator lobes. However, when the rotor passes through a "dead" point – i.e., when a rotor tooth fully seats in a stator groove – the number of contact lines increases by one, which induces DF pulsations that generate axial vibrations of the PDM as a whole (1, 11). These must be mitigated. The system of equations describing the number of contact lines – and thereby the persistent frictional interaction within the power section – is presented below:

$$\begin{cases} \Lambda_{\min} = (l-1)z_1 + 1 \\ \Lambda_{\max} = (l-1)z_1 + 2 \end{cases} \quad (1)$$

where Λ_{max} – maximum number of contact lines of the working elements (WE) (rotor angle φ equals 0 or $2\pi/z_1$, i.e., a rotor lobe fully seats in a stator groove, the "dead" point); Λ_{min} – minimum number of contact lines ($\varphi \neq 0$, $\varphi \neq 2\pi/z_1$); l – number of WE stages; z_2 and z_1 – numbers of rotor and stator lobes, respectively.

The formulas for determining the energy characteristics of a single-screw PDM are well known and reported extensively in Russian and international literature (1, 12, 13).

In this paper, authors present the most pertinent ones – those used to determine the torque and the rotational speed of the output shaft. This is necessary because the two-section bi-rotor PDM comprises two single-screw PDM, as discussed below. The torque of a PDM can be expressed in various forms. Below are two equivalent equations for determining the motor torque (1):

$$\begin{cases} M_m = \dfrac{P_m V_m}{2\pi}\eta_m \\ M_m = M_0 P_m e^2 T \end{cases} \quad (2)$$

where P_m – pressure drop across the PDM, Pa; V_m – PDM displacement (volumetric throughput), m³/s; η_m – volumetric efficiency of the PDM, dimensionless; e – the eccentricity, m; T – stator helix (lead) pitch, m; M_0 – specific torque corresponding to a unit-dimension helical gerotor mechanism (HGM) with (e, T), N/(Pa·m).

The quantity M_0 is defined as follows:

$$M_0 = z_2 \cdot (z_2 - 1 + c_e) \quad (3)$$

where c_e – tooth shape factor, dimensionless.

The rotational speed of a PDM at a given DF flow rate can be expressed as follows:

$$n = \frac{Q_m}{2\pi e^2 T}\omega_0 \quad (4)$$

where Q_m – volumetric flow rate of DF through the PDM WE (power section), m³/s; ω_0 – specific angular velocity, Pa·m/N.

The parameter ω_0 is defined by:

$$\omega_0 = \frac{1}{M_0} \quad (5)$$

From the equations it follows that the specific torque M_0 depends only on the design characteristics of the WE. Meanwhile, as seen from Equations 2-5, at a constant DF flow rate the torque and the rotational speed are independent. This design feature of the PDM underpins its key advantages:

1) Varying the WE lead (number of starts) makes it possible to adjust bit RPM and flow rate, as well as the inherently stiff torque-load characteristic of the PDM.

2) By changing the length of the power section, one can tune the primary drilling modes and the steerability of the BHA.

3) The sealing of the helical gerotor mechanism (HGM) cavities at the WE interface provides relatively effective surface control of bit load as a function of the motor pressure drop.

Figure 1 shows a typical PDM characteristic curve of rotational speed and linearized pressure drop across the PDM as functions of the developed torque. The four principal operating regimes are: no-load (n = max, M = 0), optimal (η = max), extreme (N = max) and braking/stall (n = 0; M = max). The most hazardous regime is stall (the red point «1» in Figure 1): once the motor enters this mode, the PDM rotor ceases to rotate, is forced against the stator liner and bends, while DF bypasses freely between the rotor and stator. As a result, the stator elastomer wears rapidly and the overall efficiency of the PDM deteriorates (14).

A combined drilling mode (rotating the DS while the PDM is running) and a motorized RSS (including both the PDM and the RSS in the BHA) are of particular interest, because in these modes a dynamic module is formed – namely, the rotating housing of the PDM or the RSS. This phenomenon is equivalent to the bi-rotary mechanism discussed below.

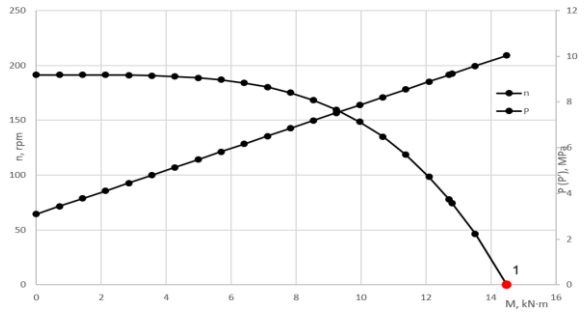

Figure 1. PDM DGR-172.5/6.61 performance curve (Q_m = 31,9 m³/s)

The combined (motor-rotary) method is a drilling technique that uses a hydraulic downhole motor (mud motor, PDM) together with surface rotation of the DS. When a PDM is used, its housing rotates.

However, due to the high stress-strain state of the drillpipe and the inability to build angle, this drilling method is not an optimal solution for well construction under a range of geologic and technical conditions.

Even so, the combined method remains relevant because it enables azimuthal orientation of the RSS and reduces frictional interaction between the DS and the borehole wall (as low as 5 rpm is sufficient), thereby improving the efficiency of directional drilling in wells with a large step-out (departure from vertical) (15).

Externally, the motor then resembles a screw-type reducer. Baldenko and Baldenko (16) referred to this mechanism as "bi-rotary". For this process to occur, the following equality must be satisfied:

$$\omega_{DC} = z_2 \omega_r \quad (6)$$

where ω_{DC} – angular velocity of DS rotation, s^{-1}, and ω_r – absolute rotational speed of the PDM rotor, s^{-1}.

In the machine proposed by the authors, termed a "two-section bi-rotor PDM" or "two-section PDM with a bi-rotary mechanism", this condition may not be met; however, the stator's rotational speed must not be zero. Accordingly, the authors adopt from Baldenkos' bi-rotary mechanism as the classical case.

A motorized RSS is a modern system for stable, precise drilling of directional wells. It consists of a hydraulic downhole motor (often a PDM) and the RSS, with the motors' output shaft driving the RSS housing (17). Its main drawbacks are: additional dynamic loading due to the flexible shaft, a relatively low maximum dogleg capability and rapid wear of the steering pads. Here and below, the terms "lower" and "upper" refer to the motors' positions along the DS, with the "lower" end being at the bit.

Motors comprising multiple power sections are well known. The most common are sectional PDMs, referred to here as "classical", whose rotors are connected in series by transmission shafts (cardan or torsional/flexible). In some cases, the rotors are phased oppositely (in antiphase), which partially mitigates the motors' radial forces (1). It is important that the orbital (transport) speeds of the coupled rotors (the rotation of the rotor axes about the stator axes) be equal; otherwise, the compensation of radial forces generated in the power sections will be nonuniform.

In such motors, at the output shaft of the lower motor the torques generated in the power sections are summed, subject to losses associated with additional inflow of DF into, and outflow from, the PDM working chambers – a drawback inherent to all sectional PDMs. The rotational speeds of a classical sectional PDM do not add; in practice, the operating speed is taken as the higher of the individual motor speeds. These motors are used with torque-intensive rock-cutting tools.

It should be noted that one of the most critical stages in designing a classical sectional PDM is the calculation of the connection assemblies (universal joints and flexible shafts). The most critical section is the lower transmission shaft, which carries both the axial loads and the torque from the two power sections. Although the physics of a sectional PDM operating with a bi-rotary mechanism differs from the classical case, as will be discussed in due course. It is essential to account for the features of the classical mechanism, since they impose specific considerations on the operating theory of the proposed motor (18).

Thus, the two-section bi-rotor PDM incorporates elements of the following technologies and techniques: PDMs, turbodrills, combined (motor-rotary) drilling, motorized RSS, as well as the classical bi-rotary mechanism and the sectional PDM with transmission coupling between the rotors.

A number of inventions are used as prototypes for the motor underlying the proposed drilling technology.

A counter-rotating turboscrew motor (TSM) invented by Morozov and Sysoev (19): in this design, a turbodrill (a dynamic motor) is installed above a PDM, with the turbodrill's output shaft connected to the housing of the PDM. A threaded connection is provided on the housing of the lower motor (the PDM) to incorporate a reamer into the BHA. The principal drawback of this invention is the use of a turbodrill; because its turbine stages are not mechanically coupled, the upper motor often ceases to operate, and the TSM functions only due to the PDM (19).

An invention by Smith (20), a motor comprising two PDMs, is also bi-rotary in principle. However, when drilling with this tool, the DS must be rotated to the right (clockwise as viewed looking at the bit), while the output shaft of the upper motor, connected to the housing of the lower motor, rotates to the left due to the right-hand helix of the upper PDM's WE. There exists a combination of DF flow rate and DS rotation speed (from the rotary table or top drive) at which the housing of the lower motor stops, or, as the author writes, "almost" stops, rotating. The RSS tool can be installed in the bore of the lower motors' transmission section to build trajectory while the DS is rotating; this is the stated technical result of the invention. The main drawback is that the two PDMs rotate in opposite directions, which can lead to thread back-off. Another drawback is the inability to operate without DS rotation.

Moreover, the upper motor contributes little to improving overall drilling efficiency: apart from enabling trajectory build in the combined mode, it mainly increases the axial load generated in the BHA, which merely allows a reduction in the amount of heavy-weight drillpipe (HWDP) required in the vertical section of the

DS, thereby reducing or eliminating sinusoidal and helical buckling (21, 22).

An invention by Baldenko, also comprising two PDMs, is of interest. In this design, a special non-rotating shroud is mounted on the lower power section, while the housing of the PDM, connected to the output shaft of the upper motor, rotates accordingly (23). The WE of both motors have a left-hand helix. The technical result is an increased output-shaft speed, enabling the use of certain diamond bits. An eccentric stabilizer may also be mounted on the housing of the lower motor to provide dogleg capability.

The two-section bi-rotor PDM consists of two PDMs. Their configurations and WE parameters may differ, which determines the machines' energy characteristics. The output shaft (spindle) of the upper motor is connected to the housing of the lower motor. A crossover sub can be used for this purpose due to the large difference in component diameters. A general view of the two-section bi-rotor PDM is shown in Figure 2. The principal advantage of the two-section PDM with a bi-rotary mechanism is the ability to build trajectory while the housing of the lower motor is rotating (with the RSS placed in the transmission section of the upper PDM). Another advantage is the increased axial load generated within the BHA. In addition, rotation of the lower motor housing reduces frictional interaction with the borehole wall (lowering contact drag due to torsional motion of the housing) and enables influence over the dynamic processes. A higher output-shaft speed with a largely preserved torque characteristic increases power at the bit, which can improve rate of penetration and allows the use of certain diamond bits. The main drawback is the need to match the operating characteristics of both motors to ensure efficient joint operation. Thus, the proposed two-section bi-rotor PDM, whose WE have left-hand helixes, features a rotating housing on the lower motor, referred to as the dynamic module.

2. MATERIALS AND METHOD

Mathematical modeling of the energy characteristics of a two-section bi-rotor PDM:

Since the sections are coupled rotor-to-stator rather than rotor-to-rotor, and if all torques arising from frictional interactions of the WE are neglected, specifically, contact of the housing with the borehole wall, inertial effects, the intrinsic material properties, and the joints between machine components, the torque at the output shaft of the two-section PDM, at the bit, is determined from the following relation:

$$\begin{cases} M_b = M_{\text{m.1}} \\ M_b = M_{\text{m.2}} \end{cases} \tag{7}$$

where M_{b} – bit torque, N·m; $M_{\text{m,1}}$ – ideal torque of the upper PDM, N·m; $M_{\text{m,2}}$ – ideal torque of the lower PDM, N·m.

For a simplified representation of the physics, the motor's reaction torque is taken equal to its ideal torque. From Equation 7, if the torque on the upper PDM is lower than the reaction torque of the lower PDM, equality between them is achieved by increasing the torque of the upper PDM. Conversely, if the torque of the upper PDM exceeds the reaction torque of the lower PDM, equality is achieved by increasing the torque of the lower PDM. The bit torque (i.e., the torque at the output shaft of the two-section PDM) assumes the value of this steady-state equality. Figure 3 presents a schematic of the proposed PDM with the characteristics used in the mathematical model indicated. The following equation serves as the basis for formulating a more detailed system of equations to determine the torques generated in the two-section PDM with a bi-rotor operating principle. The formulation explicitly accounts for a dedicated crossover sub installed between the two PDMs. Accordingly, starting from Euler's equation for a rigid body with one degree of freedom (equivalently, Newton's second law for rotational motion), augmented by linear viscous damping and torsional elasticity (24-26), we obtain the following relation:

$$J\ddot{\theta} + B\dot{\theta} + K\theta = \tau \tag{8}$$

where J – moment of inertia of the specified PDM element, kg·m²; B – viscous loss coefficient (Rayleigh dissipation, Couette flow), N·m·s/rad; K – torsional stiffness of the node, N·m/rad; τ –system output torque, N·m; θ – twist angle, deg; $\dot{\theta}$ – angular velocity, rad/s; and $\ddot{\theta}$ – angular acceleration, rad/s².

Newton's second law for rotational motion is represented by the first term on the left-hand side of Equation 8. Linear viscous damping corresponds to the second term on the left-hand side of Equation 8. The external torques are represented by the third term on the left-hand side of Equation 8.

The subscript "*r*" denotes the rotor, "*h*" the housing of the lower PDM (the dynamic module), "*m*" the motor,

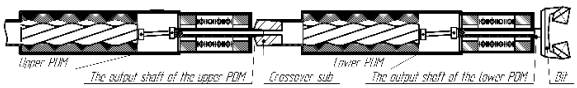

Figure 2. General view of the two-section bi-rotor PDM

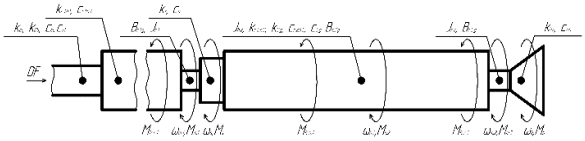

Figure 3. Computational schematic for determining the power-performance characteristics of a two-section PDM with a bi-rotary mechanism

"*s*" the crossover sub, and "*d*" the bit. The index "1" refers to the upper PDM, and "2" to the lower PDM. The kinetic energy of the rotor of the upper PDM, determined by its twist acceleration, is given by:

$$E_{kin} = \frac{1}{2}(mv_C^2 + J_C\omega_{rel.r}^2) \tag{9}$$

where v_C – rotor's linear velocity (Equation10), m/s; ω_{rel} – rotor's relative angular velocity (rotation about its own axis), s^{-1}; J_C – rotor's polar moment of inertia about its own axis (Equations 11-13), kg·m². The first term in Equation 9 corresponds to the inertia moment arising from the rotor's transport motion, while the second, and dominant, term corresponds to the relative rotation of the rotor (27).

$$v_C = \omega_r z_2 e \tag{10}$$

$$J_C = \frac{J_P}{z_1^2} \tag{11}$$

where J_P – equivalent (reduced) moment of inertia of the helical rotor undergoing planetary motion, kg·m²; ωr – rotor's absolute angular velocity, s^{-1}.

The rotor's moment of inertia about its own axis can be obtained from:

$$J_C\ddot{\theta} = F_e e - F_c h \tag{12}$$

where F_g – resultant vector of radial hydraulic forces, N; F_{res} – force that generates the resisting torque (determined by linear viscous damping and the torsional elasticity of the machine elements), N; h –lever arm of F_s, m.

Alternatively, by the Steiner (Huygens) theorem:

$$J_C = J_P + me^2 \tag{13}$$

One may also account for the moments of inertia of the spindle shaft and the bit; in that case, the total moment of inertia is given by:

$$J = J_P + J_{sh} \tag{14}$$

where J_{sh} –moment of inertia of the spindle shaft and the bit, kg·m².

The moments of inertia of the elements of the two-section PDM are determined by differentiating their kinetic energy characteristics according to Equation 9, with generalized inertial moments duly accounted for:

$$\begin{cases} \frac{d}{dt}(\frac{\partial E_{кин}}{\partial \omega_{p.1}}) = J_{p.1}\cdot\dot{\omega}_{p.1} \\ \frac{d}{dt}(\frac{\partial E_{кин}}{\partial \omega_{к.2}}) = J_{к.2}\cdot\dot{\omega}_{к.2} \\ \frac{d}{dt}(\frac{\partial E_{кин}}{\partial \omega_{p.2}}) = J_{p.2}\cdot\dot{\omega}_{p.2} \end{cases} \tag{15}$$

Viscous (velocity-dependent) losses in a PDM, arising from bearings, seals, the DF, and other sources, for engineering calculations may be taken as:

$$B = \frac{\partial M_{loss}}{\partial \omega} \tag{17}$$

where M_{loss} – torque expended on viscous losses, N·m.

In the annular clearance (annulus), for laminar flow, the viscous loss at the walls of the rotating housing of the lower motor (dry friction is accounted for separately by M_{fr} in Equation 27 is given by Pierson et al. (28):

$$B_{l.h.2} = 2\pi\mu L_{h.2}\frac{R_{h.2}^3}{g} \tag{17}$$

where μ – dynamic viscosity of the DF, Pa·s; $L_{h.2}$ – length of the housing of the lower motor (dynamic module), m; $R_{h.2}$ – radius of the housing of the lower motor, m; g – gravitational acceleration, m/s².

For turbulent flow (an increase in the viscous-friction coefficient by approximately $2\omega_{h.2}$ times) (28):

$$B_{t.h.2} = 4\pi\mu L_{h.2}\omega_{h.2}\frac{R_{h.2}^3}{g} \tag{18}$$

It is also necessary to account for viscous damping c between mechanically coupled machine elements. An important distinction from the element-wise viscosity parameter B is that c is used to compute viscous losses as the product of the relative velocity – that is, the difference in velocities of the connected moving elements. Accordingly, the Rayleigh dissipation function (29), which characterizes the aggregate viscous (hydraulic) losses in the two-section bi-rotor PDM, at the interface between the two motors takes the form:

$$\begin{aligned} R_{el} &= \frac{1}{2}(B_{r.1}\omega_{r.1}^2 + B_{h.2}\omega_{h.2}^2 + B_{r.2}\omega_{r.2}^2) + \\ &+\frac{1}{2}c_s\cdot(\omega_{r.1} - \omega_{h.2})^2 \end{aligned} \tag{19}$$

where c_s – viscous (velocity-dependent) damping in the crossover sub, N·m·s/rad.

The partial derivatives of this expression (with respect to the angular velocities of the principal elements of the PDM) are obtained as follows:

$$\begin{cases} \frac{\partial R_{el}}{\partial \omega_{r.1}} = B_{r.1}\omega_{r.1} + c_s\cdot(\omega_{r.1} - \omega_{h.2}) \\ \frac{\partial R_{el}}{\partial \omega_{h.2}} = B_{h.2}\omega_{h.2} - c_s\cdot(\omega_{r.1} - \omega_{h.2}) \\ \frac{\partial R_{el}}{\partial \omega_{r.2}} = B_{r.2}\omega_{r.2} \end{cases} \tag{20}$$

The torsional stiffness of the assembly:

$$k = \frac{GJ^{'}}{L} \tag{21}$$

where G – shear modulus, MPa; J' – polar moment of area, m⁴; and L – element length, m.

From the torsional stiffness of the crossover sub installed between the two motors, the potential energy of their connection can be determined

$$E_{pot} = \frac{1}{2} k_s (\theta_{r.1} - \theta_{h.2})^2 \tag{22}$$

where k_p – torsional stiffness of the crossover sub, N·m/rad.

In Equation 29 only the torsional stiffness of the crossover sub is taken into account. Subsequently, we account for the stiffnesses of the WE of the upper PDM and the lower PDM, the contact of the lower PDM housing with the borehole wall, the bit-rock interaction, and the DS stiffness up to the wellhead (Equation 30). To determine the twisting torque contributed by the stiffness of each element, one must take the derivative of its potential energy with respect to the twist angle. Accordingly, the following system of equations is obtained for the elements of the proposed motor

$$\begin{cases} \dfrac{\partial E_{pot}}{\partial \theta_{r.1}} = k_s \cdot (\theta_{r.1} - \theta_{h.2}) \\ \dfrac{\partial E_{pot}}{\partial \theta_{h.2}} = -k_s \cdot (\theta_{r.1} - \theta_{h.2}) \\ \dfrac{\partial E_{pot}}{\partial \theta_{r.2}} = 0 \end{cases} \tag{23}$$

Building on the preceding assumptions, a system of torque-balance equations can be formulated for the rotor system of the upper PDM, the dynamic module (housing of the lower PDM), and the rotor system of the lower PDM. Equation 8 serves as the foundation. Accordingly, the equation for the rotor system of the upper motor is derived from

$$J_{r.1}\dot{\omega}_{r.1} = M_{m.1} - M_s - B_{r.1}\omega_{r.1} - M_{fr.r.1} \tag{24}$$

where $M_{fr,r,1}$ – torque generated by contact friction in the WE of the upper PDM, N·m.

Torque balance in the dynamic module of the two-section PDM with a bi-rotary mechanism:

$$J_{h.2}\dot{\omega}_{h.2} = M_s - M_{m.2} - B_{h.2}\omega_{h.2} - M_{fr.h.2} \tag{25}$$

where $M_{fr,h,2}$ – torque generated by contact friction at the interface between the dynamic module (housing) of the lower PDM and the borehole wall, N·m.

Torque balance in the rotor system of the lower PDM

$$J_{r.2}\dot{\omega}_{r.2} = M_{m.2} - M_b - B_{r.2}\omega_{r..2} - M_{fr.r.2} \tag{26}$$

where $M_{fr,r,2}$ – torque generated by contact friction in the WE of the lower PDM, N·m.

Thus, Equations 24-26 form system that characterizes the torque behavior of the two-section PDM under a non-stabilized operating regime

$$\begin{cases} J_{r.1}\dot{\omega}_{r.1} = M_{m.1} - M_s - B_{r.1}\omega_{r.1} - M_{fr.r.1} \\ J_{h.2}\dot{\omega}_{h.2} = M_s - M_{m.2} - B_{h.2}\omega_{h.2} - M_{fr.h.2} \\ J_{r.2}\dot{\omega}_{r.2} = M_{m.2} - M_b - B_{r.2}\omega_{r.2} - M_{fr.r.2} \end{cases} \tag{27}$$

It is important to note that the reaction torque, although not explicitly present in Equations 24-27, is accounted for through energy dissipation within the proposed motor system. The crossover sub is modeled as a viscoelastic element with torsional stiffness k_s and viscous coefficient c_s (frictional torque in the sub is neglected). Its twisting torque is given by:

$$M_s = k_s \cdot (\theta_{r.1} - \theta_{h.2}) + c_s \cdot (\omega_{r.1} - \omega_{h.2}) \tag{28}$$

By substituting the obtained expressions (systems of Equations 15, 20, and 23) together with the external applied torques into the Lagrange equation, the correctness of the derived system for determining the torque forces generated in the two-section bi-rotor PDM. It can be written in matrix form as follows:

$$\underbrace{\begin{bmatrix} J_{r.1} & 0 & 0 \\ 0 & J_{h.2} & 0 \\ 0 & 0 & J_{r.2} \end{bmatrix}}_{J} \ddot{\theta} + \underbrace{\begin{bmatrix} B_{r.1} + c_s & -c_s & 0 \\ -c_s & B_{к.2} + c_s & 0 \\ 0 & 0 & B_{r.2} \end{bmatrix}}_{B} \dot{\theta} + \underbrace{\begin{bmatrix} k_s & -k_s & 0 \\ -k_s & k_s & 0 \\ 0 & 0 & 0 \end{bmatrix}}_{K} \theta = \underbrace{\begin{bmatrix} M_{m.1} - M_{fr.r.1} \\ -M_{m.2} - M_{fr.к} \\ M_{m.2} - M_{д} - M_{fr.r.2} \end{bmatrix}}_{\tau} \tag{29}$$

With the additional stiffness, viscous parameters of the system included, Equation 29 takes the following form:

$$\underbrace{\begin{bmatrix} c_s + c^{eq}_{r.1.h.1} + B_{r.1.g} & -c_s & 0 \\ -c_s & c_s + c_{r.2.h.2} + c_{h.2.g} + B_{h.2.g} & -c_{r.2.h.2} \\ 0 & -c_{r.2.h.2} & c_{r.2.h.2} + c_{b.g} + B_{r.2.g} \end{bmatrix}}_{K} \dot{\theta} + \underbrace{\begin{bmatrix} J_{r.1} & 0 & 0 \\ 0 & J_{h.2} & 0 \\ 0 & 0 & J_{r.2} \end{bmatrix}}_{J} \ddot{\theta} + \underbrace{\begin{bmatrix} k_s + k^{eq}_{r.1.h.1} & -k_s & 0 \\ -k_s & k_s + k_{r.2.h.2} + k_{h.2.g} & -k_{r.2.h.2} \\ 0 & -k_{r.2.h.2} & k_{r.2.h.2} + k_{b.g} \end{bmatrix}}_{K} \theta = \underbrace{\begin{bmatrix} M_{m.1} - M_{fr.r.1} \\ -M_{m.2} - M_{fr.h} \\ M_{m.2} - M_b - M_{fr.r.2} \end{bmatrix}}_{\tau} \tag{30}$$

where $c^{eq}_{r.1.h.1}$ and $k^{eq}_{r.1.h.1}$ – equivalent viscous parameter and stiffness of the WE of the upper PDM relative to the anchored stator (rock), with the stiffness of the entire DS up to the wellhead included, N·m·s/rad and N·m/rad,

respectively; $c_{\text{h.2.g}}$ and $k_{\text{h.2.g}}$ – viscous parameter and stiffness of the contact between the housing of the lower PDM and the borehole wall, N·m·s/rad and N·m/rad, respectively; $c_{\text{r.2.h.2}}$ and $k_{\text{r.2.h.2}}$ – viscous parameter of the rotor-stator interface of the lower PDM and the stiffness of its WE, N·m·s/rad and N·m/rad, respectively; $c_{\text{b.g}}$ and $k_{\text{b.g}}$ – viscous parameter and stiffness at the bit-rock contact, N·m·s/rad and N·m/rad, respectively; $B_{\text{r.1.g}}$, $B_{\text{h.2.g}}$ and $B_{\text{r.2.g}}$ – denote additional (experimentally identified) "to-ground" losses of the corresponding nodes that are not captured by c, N·m·s/rad.

The value of $k^{eq}_{r.1.h.1}$ can be obtained from

$$k^{eq}_{r.1.h.1} = \left(\frac{1}{k_{r.1.h.1}} + \frac{1}{k_{DS}}\right)^{-1} \tag{31}$$

where $k_{\text{r.1.h.1}}$ – stiffness of the working elements of the upper PDM relative to the anchored stator (the formation), N·m/rad; and k_{DS} is the DS stiffness up to the wellhead, N·m/rad.

An analogous procedure is used to determine $c^{eq}_{r.1.h.1}$.

By analogy with Equation 31, the coefficient k_{DS} includes the stiffness of the wellhead clamp, k_{cl}.

Accordingly, the torque loss acting on the PDM rotor due to the medium's viscosity can be determined experimentally. Set the rotor to a rotational speed at which $B\omega \gg M_{\text{fr}}$, then shut the drive down and record the decay of the angular velocity ω as a function of time, ω(t) (30). The coefficient B can also be evaluated by bringing a two-section bi-rotor PDM to a stabilized steady-state regime ($\dot{\omega} = 0$), in which case the left-hand side of the relations given in Equation 27 becomes zero. Once the remaining parameters have been obtained from instrumentation or from calculations, determining B poses no difficulty (1, 12, 31).

Another approach is to analyze the torque-governing relations for the PDM, from which the overall efficiency and its effect on the torque response of the elements of a two-section PDM with a bi-rotary mechanism can be derived. In particular, the reaction torques arising from losses in the power section due to rotor friction against the stator liner can be evaluated. Subsequently, the bit rotational speed and the power delivered at the bit, when coupled to the two-section PDM with a bi-rotary operating mechanism, should be examined.

The pressure drop across the two-section bi-rotor PDM and the axial load generated by hydraulics in the power sections of both stages add together, as in a conventional multi-section PDM. This is because the power sections (the motor's WE) are arranged in series, while the specific connection scheme does not affect the underlying physics of pressure drop and axial loading in a machine composed of two PDMs. However, since the flow field is perturbed at the interface between the sections, just as in classical multi-section PDMs, the overall pressure drop is not exactly equal to the sum of the individual pressure drops across each PDM; rather, it exceeds that sum by a small amount that can be neglected for engineering calculations (32). DF, its rheological and other parameters, play a high role in the PDM's power-performance characteristics (33, 34).

A noteworthy observation is the presence of torque pulsations in the proposed motor (12). These arise from a periodic variation of the pressure drop, given by the equation below, which itself varies due to the periodic change in the number of contact lines as defined by Equation 1:

$$\begin{cases} P_{\max} = \dfrac{P}{\Lambda_{\max}} \\ P_{\min} = \dfrac{P}{\Lambda_{\min}} \end{cases} \tag{32}$$

By combining the first relation from the set of Equation 2 with the system of Equation 27, the pressure drops across both individual motors, and, specifically, across the two-section PDM, can be obtained. The resulting system of equations is given below:

$$\begin{cases} \begin{cases} P_{m.2} = \dfrac{2\pi}{\eta_{m.2} \cdot V_{m.2}}(M_b + B_{r.2}\omega_{r.2} + M_{fr.r.2} + J_{r.2}\dot{\omega}_{r.2}) \\ P_{m.1} = \dfrac{2\pi}{\eta_{m.1} \cdot V_{m.1}}(M_b + B_{r.2}\omega_{p.2} + M_{fr.r.2} + \\ +B_{h.2}\omega_{h.2} + M_{fr.h.2} + B_{r.1}\omega_{r.1} + M_{fr.r.2} + \\ +J_{r.1}\dot{\omega}_{r.1} + J_{h.2}\dot{\omega}_{h.2} + J_{r.2}\dot{\omega}_{r.2}) \end{cases} \\ P = P_{m.2} + P_{m.1} + \Delta P \end{cases} \tag{33}$$

where ΔP – additional pressure drop induced by flow maldistribution between the PDM sections, Pa.

The expression for the axial load, making explicit the linear dependence on the pressure drop across the power section, has the form

$$F_{WE} = F_p + F_z = P_m \cdot (S_c + z_2 S) \tag{34}$$

where F_{r} – hydraulic component of the axial force in the PDM WE, N; F_{z} – axial component of the force arising from the helical engagement of the power section, N; S_{k} – projected area of the rotor-stator contact lines, m²; and S – is the open flow area of the WE, m².

For example, for two DGR-172.5/6.61 PDMs installed in series and neglecting the additional pressure drop ΔP, Equation 34 yields nearly 21.4 t of axial load on the power sections at a pressure drop of 4,41 MPa (10,68 t per motor). Thus, when the pressure drop in the BHA increases due to pairing the power sections, the axial force F_{WE} rises, which enables a greater maximum deviation of the wellbore trajectory from vertical.

In the ideal case, the bit RPM generated by two sectionally connected PDMs forming a bi-rotary mechanism adds algebraically. The output-shaft speed of the lower PDM can also be obtained from Equation 27. It is convenient to consider the stabilized regime $(\dot{\omega} = 0)$.

Importantly, under these conditions one must have $\omega_{r.1} = \omega_{h.2}$, otherwise, the angular difference ($\theta_{r.1} - \theta_{h.2}$) grows linearly and the torque in the crossover sub tends to infinity (Equation 28) (35, 36). Accordingly, imposing the equality between the output-shaft speed of the lower two-section motor and the bit speed gives

$$\omega_b = \omega_{r.2} = \frac{M_{m.1} - \omega_{r.1} \cdot (B_{r.1} + B_{h.2})}{B_{r.2}} - \frac{M_{fr.r.1} + M_{fr.h.2} + M_{fr.r.2} + M_b}{B_{r.2}} \quad (35)$$

The power at the bit increases as the rotational speed at the output shaft rises while its torque characteristics are preserved (ideal case), as follows from the equation corresponding to ideal operating conditions

$$N_b = M_b \omega_b \quad (36)$$

It is important to recognize that, for the same power at the bit, the efficiency of rock destruction can vary across different geological and operational conditions. For example, as the rock drillability category increases, it is necessary to increase the WOB and hence the torque at the bit, while reducing bit RPM.

The reason is that, if the rotational speed is maintained or raised as WOB increases, the reactive force exerted by the formation on the bit cutters grows, which hinders any substantial increase in the ROP and may prevent it altogether; simultaneously, tool wear intensifies. Consequently, increasing bit speed while holding the torque characteristic constant does not always enhance drilling efficiency, although it does enable the use of certain diamond bits (6, 37, 38). Using Equations 27, 33, 35, and 36, theoretical performance curves were plotted for the output-shaft rotational speed of the two-section PDM with a bi-rotor operating mechanism (consisting of two DGR-172.5/6.61 PDMs), its torque and power, as well as the motor efficiency, as shown in Figures 4 and 5. It's important that a two-section PDM torque in the range of 4,0-9,0 kN·m corresponds to its optimal operating regime. The WOB varies from 120 to 280 kN. Note that exceeding a torque of 12,7 kN·m causes the upper PDM to stall. Surpassing

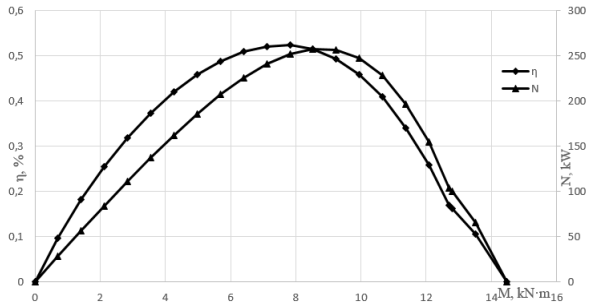

Figure 4. Plot of motor efficiency (η) and power (N) as a function of bit torque (Q_m = 31,9 m^3/s)

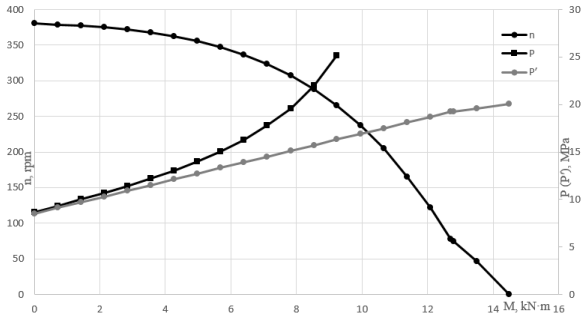

Figure 5. Plot of output-shaft rotational speed (n) and differential pressure (P, P') across the WE versus bit torque (Q_m = 31,9 m^3/s)

this critical torque and stalling the PDM is accompanied by a rise in pressure and, consequently, necessitates reducing WOB. Ensuring that the two-section PDM with a bi-rotary mechanism operates within the calculated range will enable efficient well drilling.

In Figure 5, the graph of the function $P'(M)$ provides a simplified (linearized) representation of the pressure differential characteristic across the two-section bi-rotor PDM, assuming a constant volumetric efficiency. The P(M) plot is truncated because it tends to infinity.

3. DISCUSSION AND RESULTS

After developing the mathematical model for predicting PDM performance, it must be benchmarked against field measurements. In other words, the model's accuracy should be quantified as the error of the computed parameter relative to the physically measured value. A key feature of a multi-section PDM installed in series is that the same mud flow passes through the power sections of both motors. Consequently, efficient operation of a two-section PDM requires that the rated (required) DF flow rates of the two sections be equal. If the motors are selected without regard to this constraint, the flow rate through one section may fall within its optimal operating range while the other does not, reducing the overall efficiency of the machine. Therefore, it is essential to select PDMs whose required DF rates are matched, with due consideration of their specifications. Alternatively, one may re-tune WE of one PDM or install auxiliary flow-control elements to regulate the circulating DF delivered to the volumetric motor's power section.

Another promising research direction is to treat the housing of the lower motor as a dynamic stabilization module for self-excited oscillations, that is, as a device for suppressing torsional vibrations (stick-slip) that arise at the bit during drilling. Moreover, this dynamic module can not only mitigate harmful vibrations but, if driven into resonance with them, also generate elevated oscillation levels that help free the assembly from stuck-pipe conditions and mitigate pack-off around the BHA.

Control of the dynamic module can be exercised by adjusting the DF flow rate Q, thereby avoiding changes to surface DS RPM at the rig floor or to WOB via movement of the traveling block. Table 1 summarizes the key drawbacks of the principal control methods for the dynamic module of a two-section bi-rotor PDM.

An interesting prospect is to machine a threaded profile on the rotating housing to mount a reamer, which could significantly enhance drilling efficiency.

However, because the reamer and the bit may engage formations with different drillability classes, and despite the fact that such a configuration is not uncommon in practice, this option requires careful evaluation. Specifically, mismatches in the geological conditions suitable for the reamer versus the bit can excite high-amplitude dynamic responses in the BHA (axial, radial, torsional), triggering self-excited oscillations and resonance with vibrations generated elsewhere along the DS.

An interesting prospect is to machine a threaded profile on the rotating housing to mount a reamer, which could significantly enhance drilling efficiency. However, because the reamer and the bit may engage formations with different drillability classes, and despite the fact that such a configuration is not uncommon in practice, this option requires careful evaluation.

Mismatches in the geological conditions suitable for the reamer versus the bit can excite high-amplitude dynamic responses in the BHA (axial, radial, torsional), triggering self-excited oscillations and resonance with vibrations generated elsewhere along the DS.

TABLE 1. Key drawbacks of the principal methods for regulating PDM power-performance characteristics

Methods for controlling the dynamics of the lower motor housing	Key drawback
Adjusting axial load at the bit (WOB)	For extended wells, because of multiple sinusoidal and spiral bends of the DS, raising the string at the wellhead to change WOB may require hoisting several meters of pipe
Adjusting DS rotation (surface RPM at the wellhead)	The DS acts as a torsional spring; thus transmission of surface rotation to the BHA is imperfect, especially over long intervals. High DS-wellbore friction leads to stick-slip
Adjusting drilling-mud flow rate	Requires maintaining an RPM-torque characteristic consistent with an efficient drilling regime

4. CONCLUSION

A two-section PDM with a bi-rotary mechanism is proposed. The assembly consists of two rigidly coupled gerotor stages and a crossover sub that connects the output shaft of the upper PDM to the housing of the lower PDM, enabling efficient directional and horizontal drilling with a bent-housing motor assembly. Additionally, more precise mathematical modeling is required for the stall (braking) torque of one of the motors, the discontinuity (jump) in its power/energy characteristics, and the subsequent operation of the two-section PDM with a bi-rotary mechanism. The operating principle is described, the advantages are identified, and a drilling methodology using the proposed motor is developed. Prototypes and analogs of existing designs are noted: a motorized RSS, a two-section PDM with a right-hand helical profile in the upper power section, and a two-section PDM with a stationary shroud on the lower motor. Their benefits and limitations are highlighted. The characteristics of a conventional PDM and its specific features are outlined. The system's nonlinearity is substantiated, together with its key distinctions from a classical multi-section PDM (where the rotors are interconnected by a transmission shaft). Particular emphasis is placed on the correspondence with, as well as the fundamental differences and analogies relative to, the classical multi-section PDM.

The principal advantages and limitations of the proposed two-section PDM (bi-rotary mechanism) are highlighted, together with its technological distinctiveness. The motor should be assembled from two PDMs whose individual torques not only do not reach the stall torque of the counterpart, but also each fall within a range conducive to efficient drilling. To achieve an optimal match between the required mud flow rate of one section and the flow rate that is optimal for the other, retuning of one power section is recommended. The need to incorporate a dynamic module is also established.

Calculations were performed to determine the operating characteristics of the bi-rotor PDM – namely torque, rotational speed, power, pressure drop, and the axial load generated in the BHA. Particular attention is drawn to the possibility of only a modest increase – or no increase at all – in ROP when bit RPM is raised while preserving the torque characteristic at the bit under certain geologic and operational conditions. In evaluating the output-shaft torque of the two-section bi-rotor PDM, the inertial effects of the motor rotors and the dynamic module (the housing of the lower PDM), the viscous (damping) properties of the elements, and their stiffnesses were taken into account. The governing equation was derived and justified using Lagrange's equation; Rayleigh's dissipation function, Euler's equation for a rigid body with one degree of freedom (Newton's second law for rotational motion), the parallel-axis theorem (Steiner-Huygens) and Couette flow were also employed. Directions for further investigation of the two-section bi-rotor PDM are proposed.

Acknowledgements

The authors appreciates Saint Petersburg Mining University of Empress Catherine II and the Arctic Research Center for providing the necessary facilities and support to conduct this research.

Funding

This research received no external funding.

Ethics Approval and Consent to Participate

This article does not involve any studies with human participants or animals performed by any of the authors. Therefore, ethics approval and consent to participate are not applicable.

Competing Interests

The author declares that there are no known financial or organizational conflicts of interest that could have influenced the work reported in this paper.

Data Availability

The data that support the findings of this study are available upon reasonable request.

Declaration of Generative AI and AI-assisted Technologies in the Writing Process

During the preparation of this manuscript, the author used ChatGPT exclusively for minor language editing and stylistic refinement to improve clarity and readability. The author carefully reviewed, revised, and approved the final content and takes full responsibility for the accuracy, integrity, and originality of the work.

Authors Biosketches

Mikhail Vladimirovich Dvoynikov is a Professor and Head of the Wells Drilling Department at Saint Petersburg Mining University of Empress Catherine II, and the Scientific Director of the Arctic Research Center. He holds a Dr.Sc. (Engineering/Technical Sciences) degree and his research focuses on oil and gas well drilling and completion technologies, drilling fluids, and oil and gas field development.

Dmitry Olegovich Morozov is a Ph.D. student at the Wells Drilling Department, Saint Petersburg Mining University of Empress Catherine II. His research interests include drilling equipment, well construction technologies and drilling fluids.

REFERENCES

1. Baldenko DF, Baldenko FD, Gnoevykh AN. Single screw hydraulic machines. Vol. 2. Screw downhole engines. Moscow, Gazprom Information and Advertising Center, 2007, 470. EDN QMJKHP
2. Raupov I, Rogachev M, Shevaldin E. Review of Formation Mechanisms, Localization Methods, and Enhanced Oil Recovery Technologies for Residual Oil in Terrigenous Reservoirs. Energies. 2025;18(21):5649. https://doi.org/10.3390/en18215649
3. Nutskova MV. Effect of Mineral Wool Impregnated with Carbon Nanotubes on Properties of Cement at High Temperatures. International Journal of Engineering, Transactions A: Basics. 2025;38(1):148-151. https://doi.org/10.5829/ije.2025.38.01a.14
4. Simonyants SL, Al Taee M. Stimulation of the Drilling Process with the Top Driven Screw Downhole Motor. Journal of Mining Institute. 2019;238:438-442. https://doi.org/10.31897/PMI.2019.4.438
5. Lyagov IA, Baldenko FD, Lyagov AV, Yamaliev VU, Lyagova AA. Methodology for calculating technical efficiency of power sections in small-sized screw downhole motors for the «Perfobur» system. Journal of Mining Institute. 2019;240:694-700. https://doi.org/10.31897/PMI.2019.6.694
6. Neskromnykh VV, Popova MS, Golovchenko AE, Petenev PG, Baochang L. Method of drilling process control and experimental studies of resistance forces during bits drilling with PDC cutters. Journal of Mining Institute. 2020;245:539-546. https://doi.org/10.31897/PMI.2020.5.5
7. Invention patent application №2025132209 Russian Federation. Two-section positive displacement downhole motor with a bi-rotor mechanism of action / M.V. Dvoynikov, D.O. Morozov; applicant Federal State Budgetary Educational Institution of Higher Education "Saint Petersburg Mining University". Declared 19.11.2025
8. Chuyko EV, Chetvertneva IA, Movsumzade EM, Loginova ME, Tivas NS, Giniyatullin AN. History of horizontal drilling technology development of oil and gas wells. History and Pedagogy of Natural Science. 2024;3-4:74-78. https://doi.org/10.24412/2226-2296-2024-3-4-74-78
9. Litvinenko VS, Petrov EI, Vasilevskaya DV. Assessment of the role of the state in the management of mineral resources. Journal of Mining Institute. 2023;259:95-111. https://doi.org/10.31897/PMI.2022.100
10. Blinov PA, Silichev NM, Nikishin VV, Gorelikov VG. Substantiation and development of a methodology for calculating the bending of the drive shaft of a continuous deflector for drilling with coring. SOCAR Proceedings. 2025;3:39-48. https://doi.org/10.5510/OGP20250301095
11. Sidorkin DI, Kupavykh KS. Justification on Choosing Screw Pumping Units as Energy Efficient Artificial Lift Technology. Energetika. Proceedings of CIS Higher Education Institutions and Power Engineering Associations. 2021;64(2):143-51. https://doi.org/10.21122/1029-7448-2021-64-2-143-151
12. Baldenko DF, Baldenko FD, Gnoevykh AN. Single screw hydraulic machines. Vol. 1. Single screw pumps. Moscow, Gazprom Information and Advertising Center, 2005, 488. EDN QMJKIJ
13. Kuang Y, Zhou J. Performance evaluation for positive displacement motors by combining fluid-structure interaction simulations and experiments. SPE Journal. 2025;30(1):152-68. https://doi.org/10.2118/223929-PA
14. Shi C, Wan X, Deng J, Zhu X. Research on fatigue lifetime prediction of stator rubber bushing based on rubber aged experiment. Journal of Testing and Evaluation. 2022;50(4):2209-26. https://doi.org/10.1520/JTE20200669

15. Povalikhin AS. A technology of a horizontal well drilling in case of a casing string combined rotation. Petroleum Engineer. 2019;3:5-9. EDN YEEHYT
16. Baldenko DF, Baldenko FD. Working process features and characteristics of positive displacement motors in the rotation mode of a drill string. Drilling and Oil. 2019;11:8-13. EDN YIMPTH
17. Geng H, Zhang B, Xie Y. Rotary Steerable Drilling Technology: Bottlenecks, Breakthroughs and Intelligent Trends in China Shale Gas Development. Processes. 2025;13(11):3471. https://doi.org/10.3390/pr13113471
18. Biletskyi V, Landar S, Mishchuk Y. Modeling of the power section of downhole screw motors. Mining of Mineral Deposits. 2017;11(3):15-22. https://doi.org/10.15407/mining11.03.015
19. Patent RU 2 368 752 C1. Counter-rotating turboprop engine. Morozov NS, Sysoev NI. Declared 20.05.2008. Published 27.09.2009. (In Russian). EDN LNPIMG
20. Patent US 9 771 787 B2. Multi-directionally rotating downhole drilling assembly and method. Smith G. Declared 14.10.2016. Published 26.09.2017. (In English)
21. Kunshin AA, Buslaev GV, Reich M, Ulyanov DS, Sidorkin DI. Numerical simulation of nonlinear processes in the "Thruster-Downhole Motor-Bit" system while extended reach well drilling. Energies. 2023;16(9):3759. https://doi.org/10.3390/en16093759
22. Tananykhin DS. Scientific and methodological support of sand management during operation of horizontal wells. International Journal of Engineering, Transactions A: Basics. 2024;37(7):1395-407. https://doi.org/10.5829/ije.2024.37.07a.17
23. Patent RU 2 524 238 C2. Screw downhole motor. Baldenko DF, Baldenko FD, Baletinskikh DI, Vorobyev VG, Lunev AV, Selivanov SM, Smirnov AS. Declared 17.08.2012. Published 27.07.2014. (In Russian)
24. Shi X, Jiao Y, Yang X, Liu J, Zhuo Y. Establishment of drill-string system dynamic model with PDM and influence of PDM parameters on stick-slip vibration. Arabian Journal for Science and Engineering. 2024;49:8727-39. https://doi.org/10.1007/s13369-023-08620-z
25. Ritto TG, Aguiar RR, Hbaieb S. Validation of a drill string dynamical model and torsional stability. Meccanica. 2017;52:2959-2967. https://doi.org/10.1007/s11012-017-0628-y
26. Samuel R, Baldenko DF, Baldenko FD. Mud Motor PDM Dynamics: A Control Model for Automation. IADC/SPE International Drilling Conference and Exhibition. 2022; Paper SPE-208789-MS. https://doi.org/10.2118/208789-MS
27. Samuel R, Baldenko DF, Baldenko FD. Mud Motor PDM Dynamics: An Analytical Model. SPE Annual Technical Conference and Exhibition. 2021; Paper SPE-206064-MS. https://doi.org/10.2118/206064-MS
28. Pierson JL, Kharrouba M, Magnaudet J. Hydrodynamic torque on a slender cylinder rotating perpendicularly to its symmetry axis. Physical Review Fluids. 2021;6:094303. https://doi.org/10.1103/PhysRevFluids.6.094303
29. He Y, Chen Y, Hao X, Deng S, Li C. Research on dynamic calculation methods for deflection tools in deepwater shallow soft formation directional wells. Processes. 2025;13(6):1947. https://doi.org/10.3390/pr13061947
30. Baravian C, Quemada D. Using instrumental inertia in controlled-stress rheometry. Rheologica Acta. 1998;37:223-233. https://doi.org/10.1007/s003970050110
31. Lu D, Wang M, Xu Y, Wang X. Analytical Determination of Stick–Slip Whirling Vibrations and Bifurcations in Rotating Machinery. Applied Sciences. 2024;14(16):7338. https://doi.org/10.3390/app14167338
32. Lyagov IA, Lyagov AV, Isangulov DR, Lyagova AA. Selection of the required number of circulating subs in a special assembly and investigation of their performance during drilling of radial branching channels by sectional positive displacement motors. Journal of Mining Institute. 2024;265:78-86. EDN ZBPWKU
33. Leusheva EL. Evaluation of possible application of powder made from fallen tree leaves as a drilling mud additive. International Journal of Engineering Transactions B: Applications. 2024;37:1592-1599. https://doi.org/10.5829/ije.2024.37.08b.12
34. Leusheva EL, Morozov AO, Morozov DO. Ecological biodegradable additives for improving rheological and filtration characteristics of water-based drilling mud. Perm Journal of Petroleum and Mining Engineering. 2024;24(3):120-130. https://doi.org/10.15593/2712-8008/2024.3.3
35. Rybakov DA, Dorokhin EG, Andreev KV, Buslaev GV. Development of a Hydraulic Circulation Sub as a Tool to Prevent Mud Losses During Well Drilling. International Journal of Engineering Transactions A: Basics. 2024;37(10):2091-98. https://doi.org/10.5829/IJE.2024.37.10A.19
36. Dong G, Chen P. The vibration characteristics of drillstring with positive displacement motor in compound drilling Part 2: Transient dynamics and bit control force analysis. International Journal of Hydrogen Energy. 2018;43(27):12189-12199. https://doi.org/10.1016/j.ijhydene.2018.02.198
37. Al Shekaili A, Liy Y, Papatheou E. Drilling performance analysis of a polycrystalline diamond compact bit via finite element and experimental investigations. International Journal of Rock Mechanics and Mining Sciences. 2024;182:105862. https://doi.org/10.1016/j.ijrmms.2024.105862
38. Aribowo AG, Aarsnes UJ, Chen K. Analysis of a downhole passive regulator in drilling: A distributed parameter modeling approach. Journal of Sound and Vibration. 2024;618:119300. https://doi.org/10.1016/j.jsv.2025.119300

COPYRIGHTS
©2026 The author(s). This is an open access article distributed under the terms of the Creative Commons Attribution (CC BY 4.0), which permits unrestricted use, distribution, and reproduction in any medium, as long as the original authors and source are cited. No permission is required from the authors or the publishers.

Persian Abstract

چکیده

برای حفاری چاه‌های نفت و گاز، موتورهای پیچشی پایین‌چاهی (PDM) هم در روسیه و هم در خارج از آن به‌طور گسترده به کار گرفته می‌شوند و سهم استفاده از آن‌ها بیش از ۸۰٪ است. با این حال، PDM با مجموعه‌ای از کاستی‌ها روبه‌روست که به کارایی حفاری چاه‌های مایل–جهت‌دار و فرآیند حفاری به‌طور کلی مربوط می‌شود. نخست، در اجزای کاری این موتور فرآیندهای دینامیکی نامطلوبی تولید می‌گردد که بر بهره‌وری کل عملیات حفاری اثر منفی دارد. دوم، سرعت دورانی پایین محور/شفت خروجی است که بهره‌برداری از طیفی از مته‌های الماسی را ناممکن می‌کند. سوم، نسبت کشیدگی افقی چاه به عمق عمودی آن تقریباً هرگز از ٤،٠ فراتر نمی‌رود، در حالی که برای سیستم هدایت‌پذیر چرخشی (RSS) این نسبت می‌تواند به ٦،٠ برسد. در حال حاضر، سامانه‌های RSS موتوردار و بدون موتور هرچه بیشتر به کار می‌روند و با کمک آن‌ها حفاری چاه‌هایی با بیشترین انحراف از قائم و با پروفیل مسیرِ به‌طور مشخص از پیش تعیین‌شده امکان‌پذیر است. بدیهی است که هر دوی این راه‌حل‌ها و نیز گزینه‌های دیگر، مزایا و معایب خود را دارند که پرهیز کامل از آن‌ها در جریان عملیات حفاری دشوار و گاه ناممکن است. فناوری حفاری با یک PDM دوبخشیِ دارای سازوکار دو–روتوره پیشنهاد می‌شود که امکان افزایش کارایی حفاری چاه‌های مایل–جهت‌دار را فراهم می‌کند. در این کار، نمونه‌های اولیهِ موتورِ طراحی‌شده ارائه شده، شباهت‌ها و تفاوت‌های شاخص آن با تکنیک‌ها و فناوری‌های پیشین مشخص گردیده و همچنین مشخصه‌های PDM دوبخشی–از جمله گشتاور، سرعت دورانی، توان در ابزار سنگ‌بر/مته و بار محوریِ تولیدشده در مونتاژ تحتانی رشته حفاری (BHA) –تعیین شده است. امکان تنظیم عملکرد موتور از طریق اصلاح دبی گل/سیال حفاری در بخش کاری روتور–استاتور نیز توجیه شده و محورهای بالقوه برای پژوهش‌های آینده ارائه گردیده است.